SOFT ROBOTICS
Volume 00, Number 00, 2022

DOI: 10.1089/soro.2021.0128

SoRo
Soft Robotics

Open camera or QR reader and scan code to access this article and other resources online.

Designing a Contact Fingertip Sensor Made Using a Soft 3D Printing Technique

Alejandro Ibarra,[1] Baptiste Darbois-Texier,[2] and Francisco Melo[1]

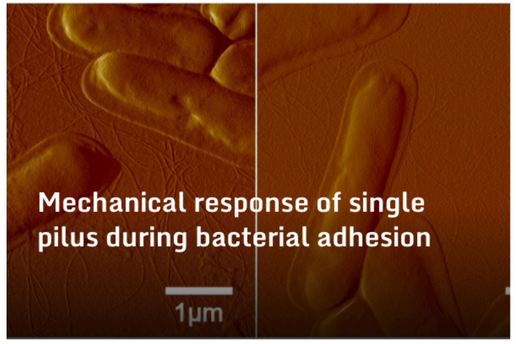

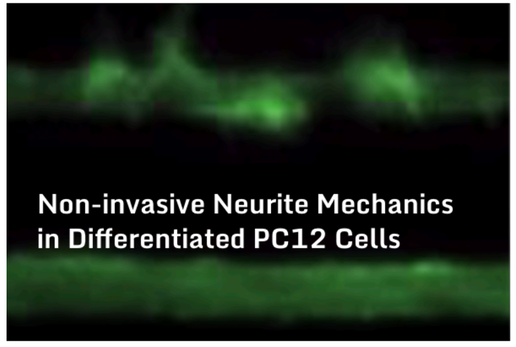

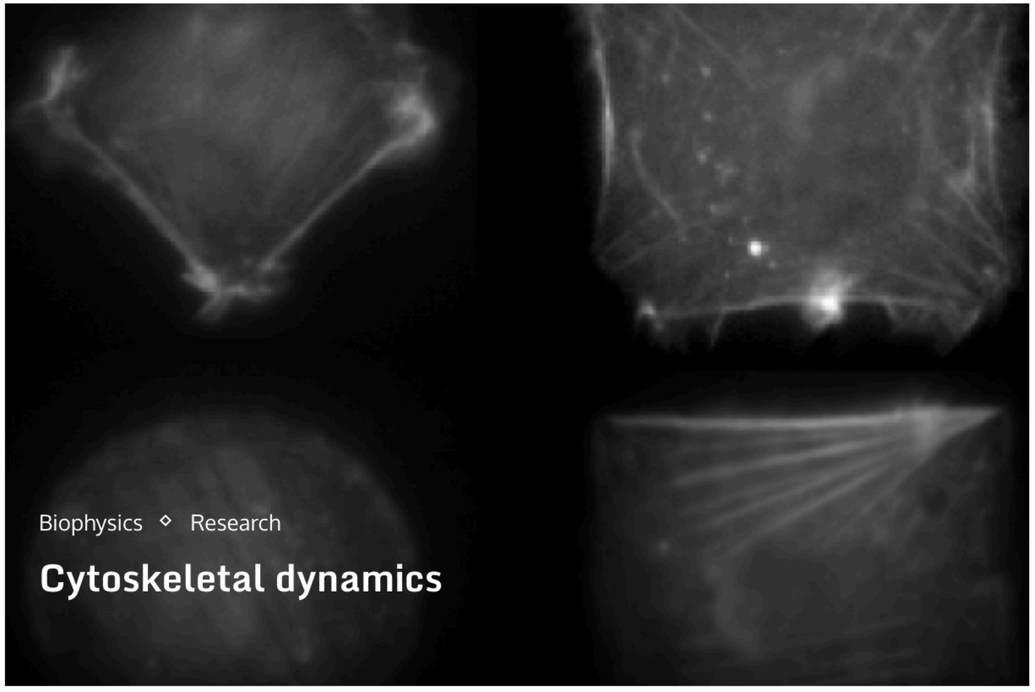

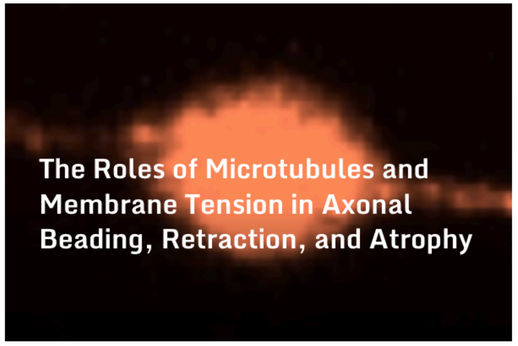

Type and hit enter...

SERVICES & RESOURCES

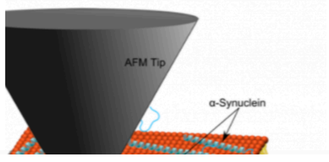

NEWS

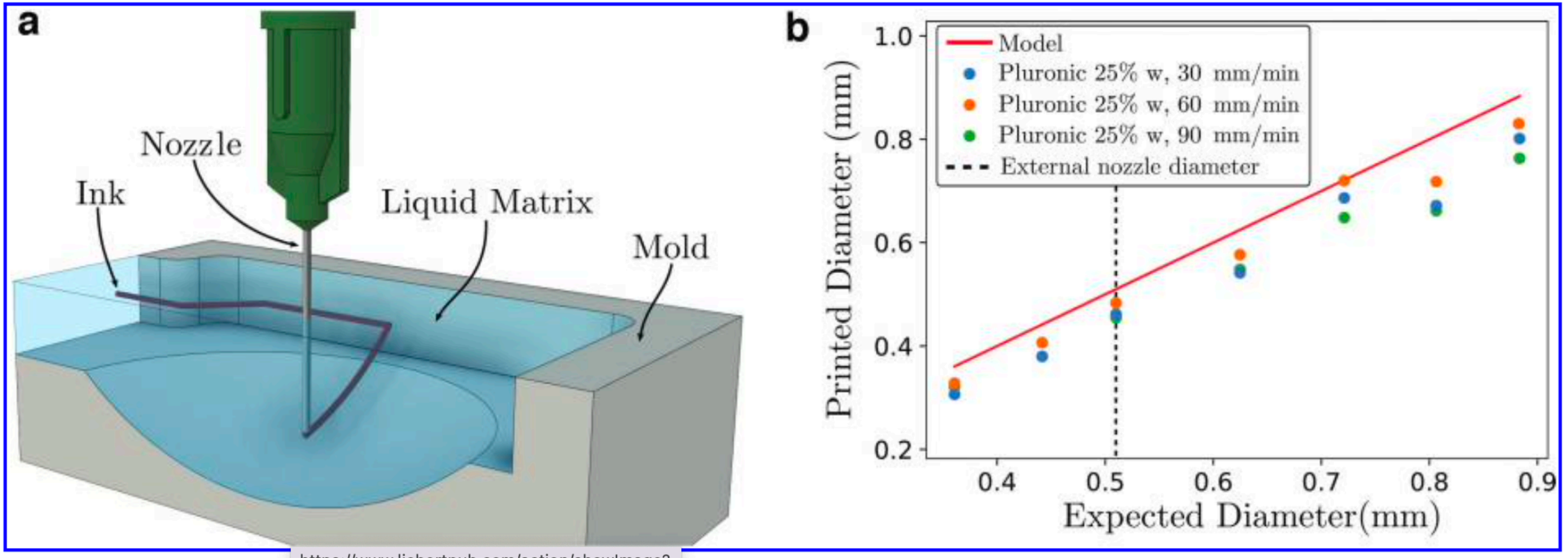

FIG. 1. **(a)** Schematic e. There are three micro controlled axes for nozzle motion, which facilitate the accurate in atrix. **(b)** Size of the injected channel as a function of the expected diameter, D_s, for a fixed nozzle diameter ($D = 0.5$ mm) marked with the *vertical dashed line* and nozzle speed. *Solid red line* indicates the prediction obtained from the rate of the deposited volume. Color images are available online.

Building the sensor - details

- The matrix is made of the commercial silicone Ecoflex (Smooth-On). Cure time is increased through the addition of Slo-jo (Smooth-On) and Thivex (Smooth-On) thixotropic agent. This procedure allows to reach working times of 20 min at room temperature (T = 20°C).

- The conductive channel is made by injecting a suspension of Aerosil 200 (Fumed Silica) to 6 %w/w in EMIM-ES (1-Ethyl-3-methylimidazolium ethyl sulfate ‡95% from Sigma-Aldrich). After mixing, the suspension is degassed and loaded into a syringe.

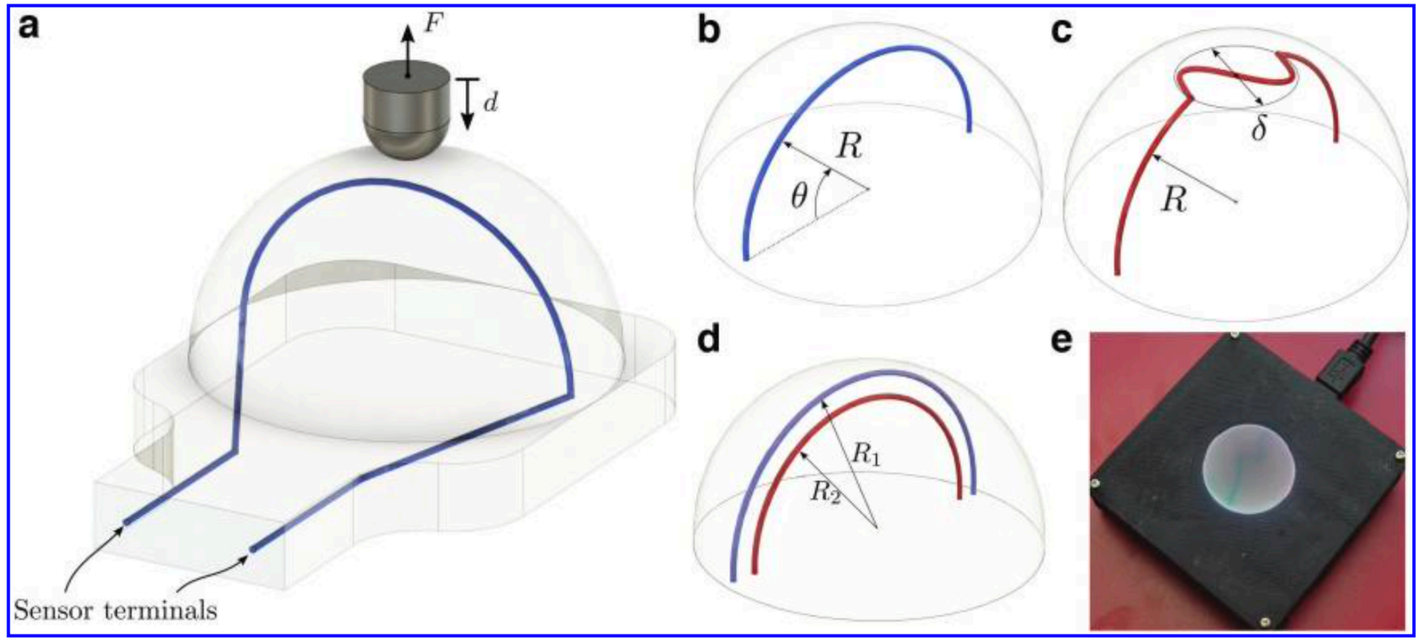

FIG. 3. **(a)** Diagram of experimental setup, showing the contact detector of $R_s = 15$ mm. **(b)** Semicircumferential sensitive element positioned at $R = 13$ mm. **(c)** Sinusoidal sensitive element, positioned $R = 13$ mm from the hemispherical center. **(d)** Multiple semicircumferential centered elements with different radii ($R_1 = 14$ mm, $R_2 = 12$ mm). **(e)** Picture of a sinusoidal sensor of 13 mm radius. Color images are available online.

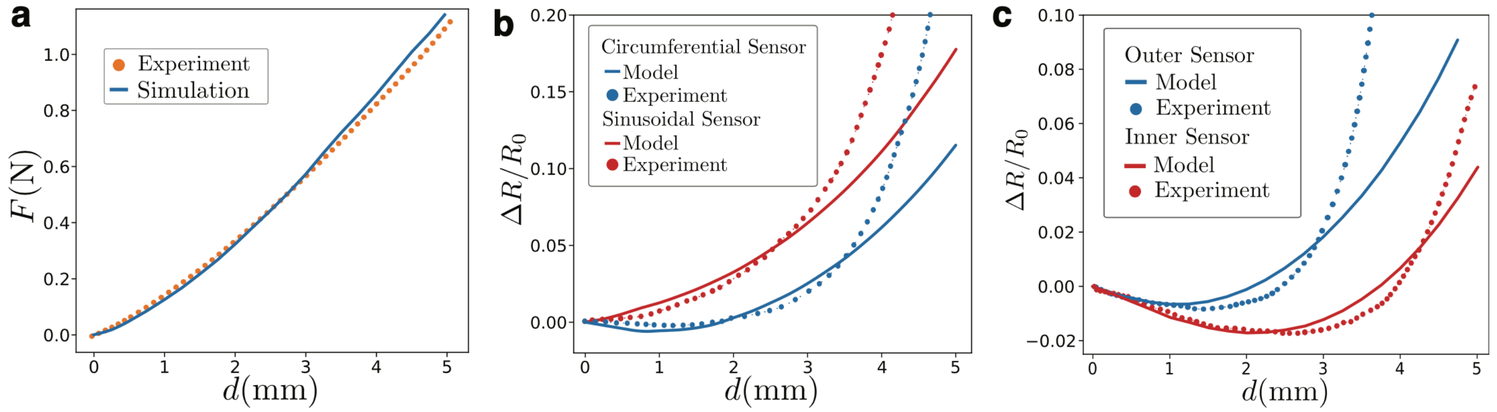

FIG. 4. **(a)** Force as a function of the indentation depth, for both the circumferential and the sinusoidal sensors. $R_s =$ 15 mm. *Orange circles* depict the observed experimental force, and the *blue line* is the predicted force from the numerical simulation. **(b)** The relative change in resistance for the semicircumference and the sinusoidal sensors. *Circles* are the experimental values, lines the numeric predictions. **(c)** Multiple semicircumferential elements of radii, $R_1 = 14$ mm, $R_2 = 12$ mm. (Parameters for the numeric are: μ=0.074 MPa and κ_0=0.1653 MPa). Color images are available online.

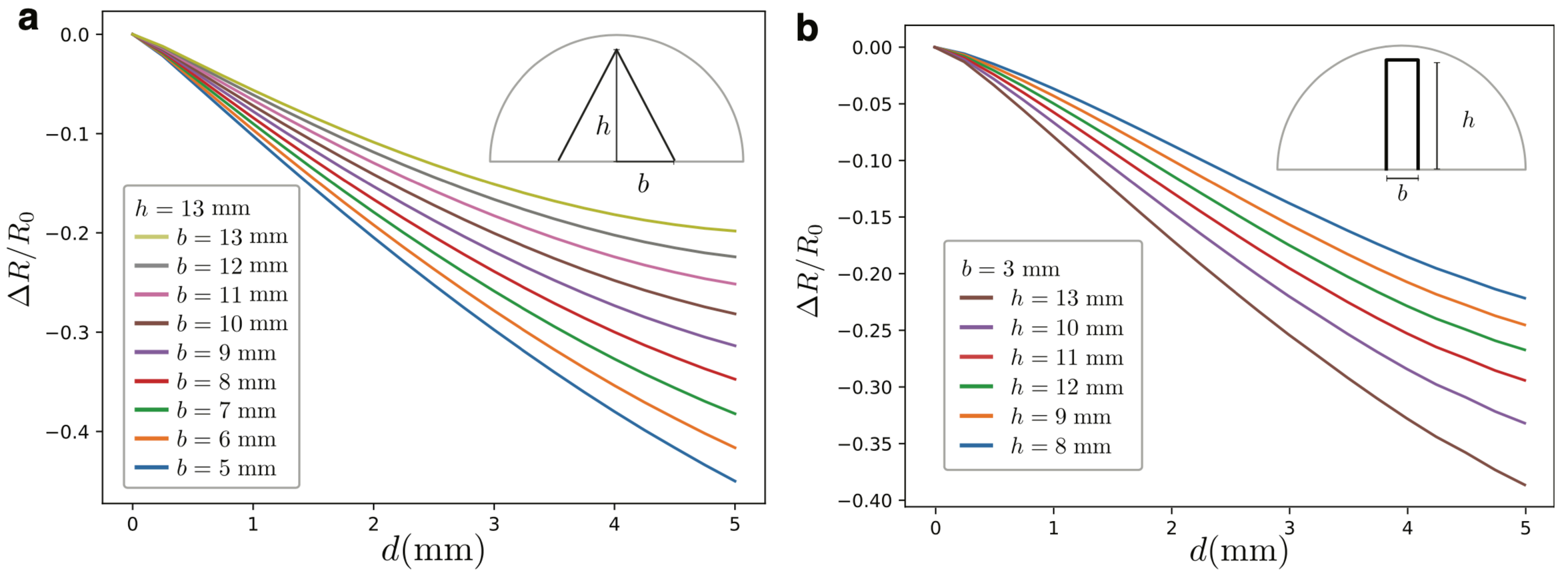

FIG. 6. Calculations of contact sensor resistance (Silicone Ecoflex), with a semispherical shape of $R_s = 15$ mm, under vertical indentation. **(a)** Triangular circuit, with a constant $h = 13$ mm, and a variable triangular base, b. Linearity and sensitivity are increased with decreasing b. **(b)** Rectangular circuit, with constant b, and variable height, h. Both linearity and sensitivity increase with increasing h. Color images are available online.

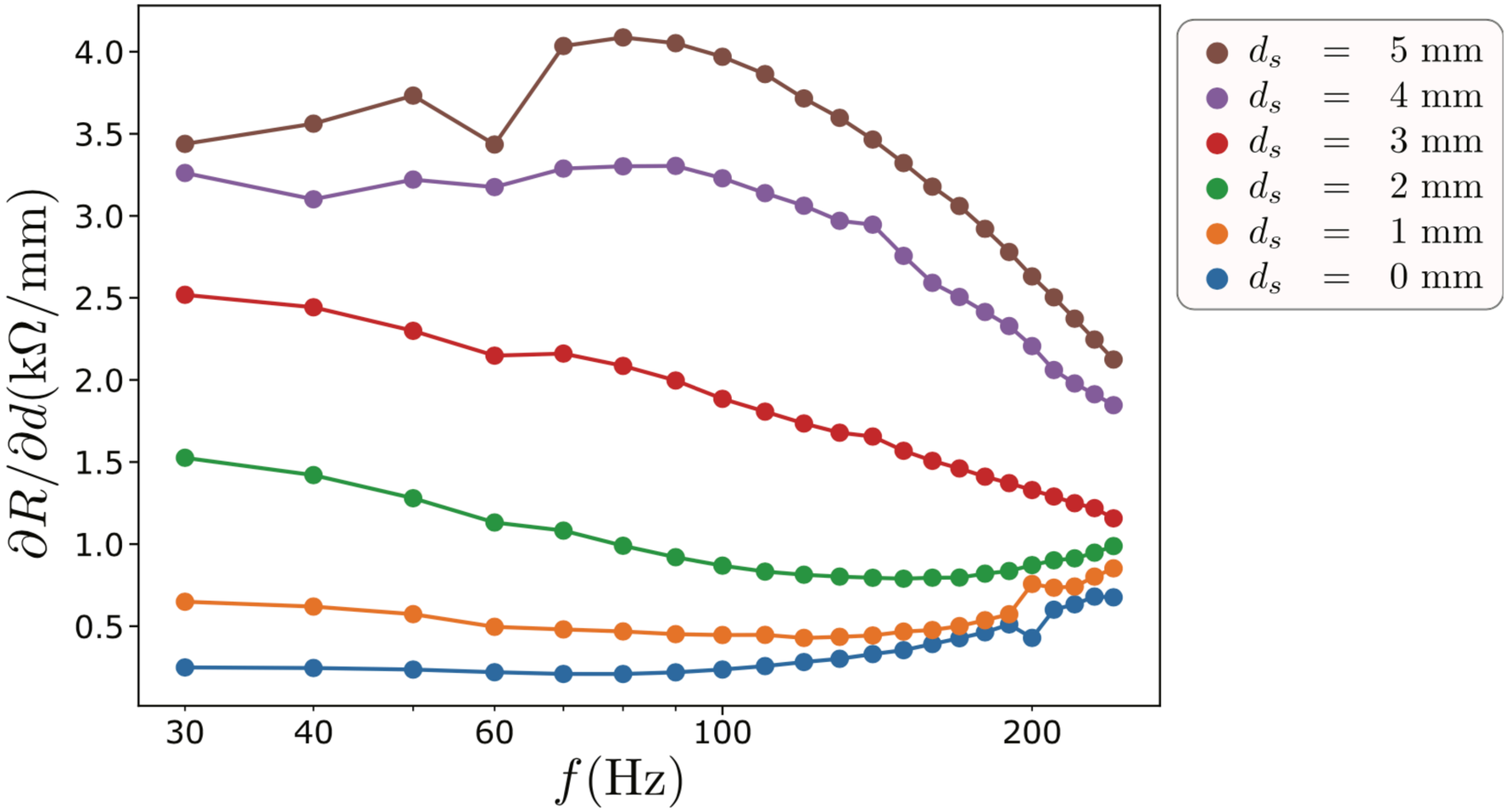

FIG. 7. Sensitivity of the resistance response, ∂R, with respect to the indentation variation, ∂d, as a function of frequency, for different indentation levels, d_s. Color images are available online.

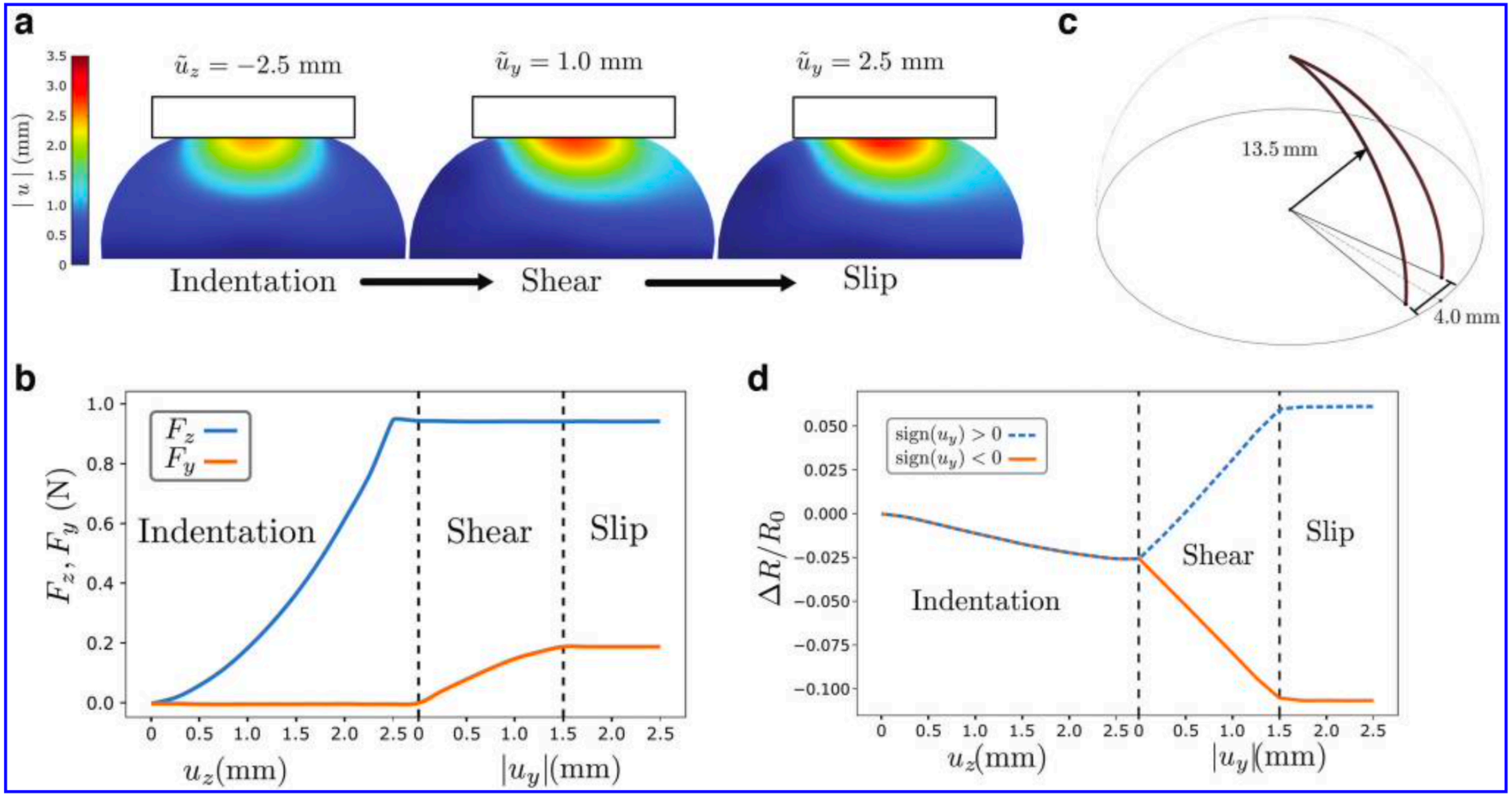

FIG. 8. **(a)** Displacement field at the vertical symmetry plane of a 15 mm radius hemispherical sensor, compressed vertically at the top by a flat surface, a distance of 2.5 mm. Color scale represents the norm of the displacement field. The indentation, the shearing, and the sliding stages are illustrated. **(b)** Force on the rigid object for the indentation and shear stage. The vertical force is *blue*, and the friction force in the horizontal direction is *orange*. The horizontal axis represents both variables, $\tilde{u}_z$ and $\tilde{u}_y$, the displacement of the rigid object and its horizontal movement, respectively. **(c)** Geometry of the proposed shear sensor, composed of a circuit of two semicircles of 90° and 13.5 mm radius, separated at the lower end by a distance of 4 mm and joined at the *top*. **(d)** Calculated electrical response for both the indentation and the shear stages is shown. The *blue segmented line* is $\tilde{u}_y > 0$, and the *orange* line is $\tilde{u}_y < 0$. Color images are available online.

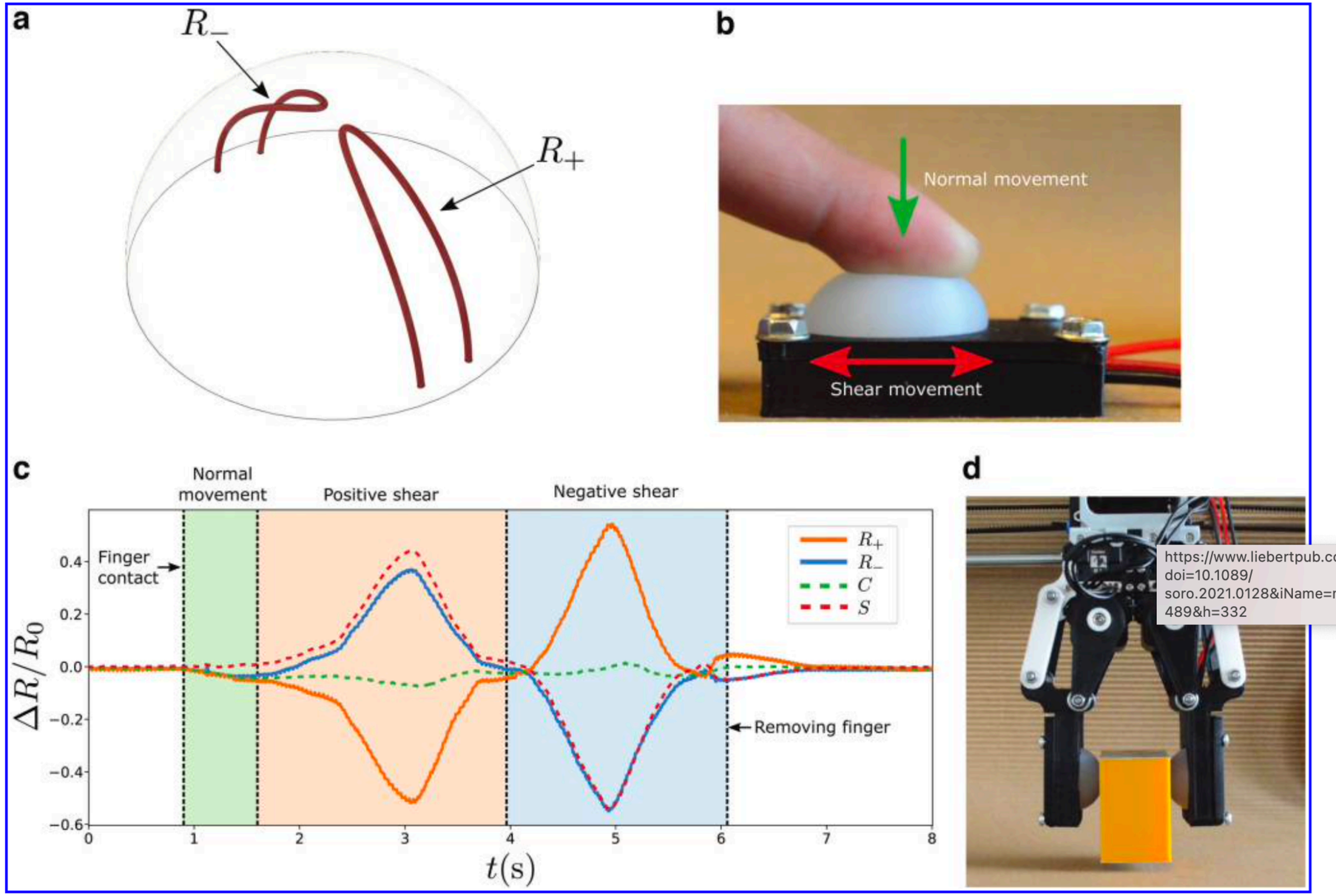

FIG. 9. **(a)** Picture of the two-quadrant sensor for the detection of the axial compression and the shear along a single axis. **(b)** Configuration schematizing the cycle used to illustrate sensor functioning: (1) compression, (2) positive shear, (3) negative shear, (4) compression released. **(c)** Direct readings, R_+ and R_- of right and left quadrants, and the calculated compression and shear, C and S, respectively, for the process described in **(b)**. **(d)** Sensor is installed in one of the arms of a gripper. Color images are available online.

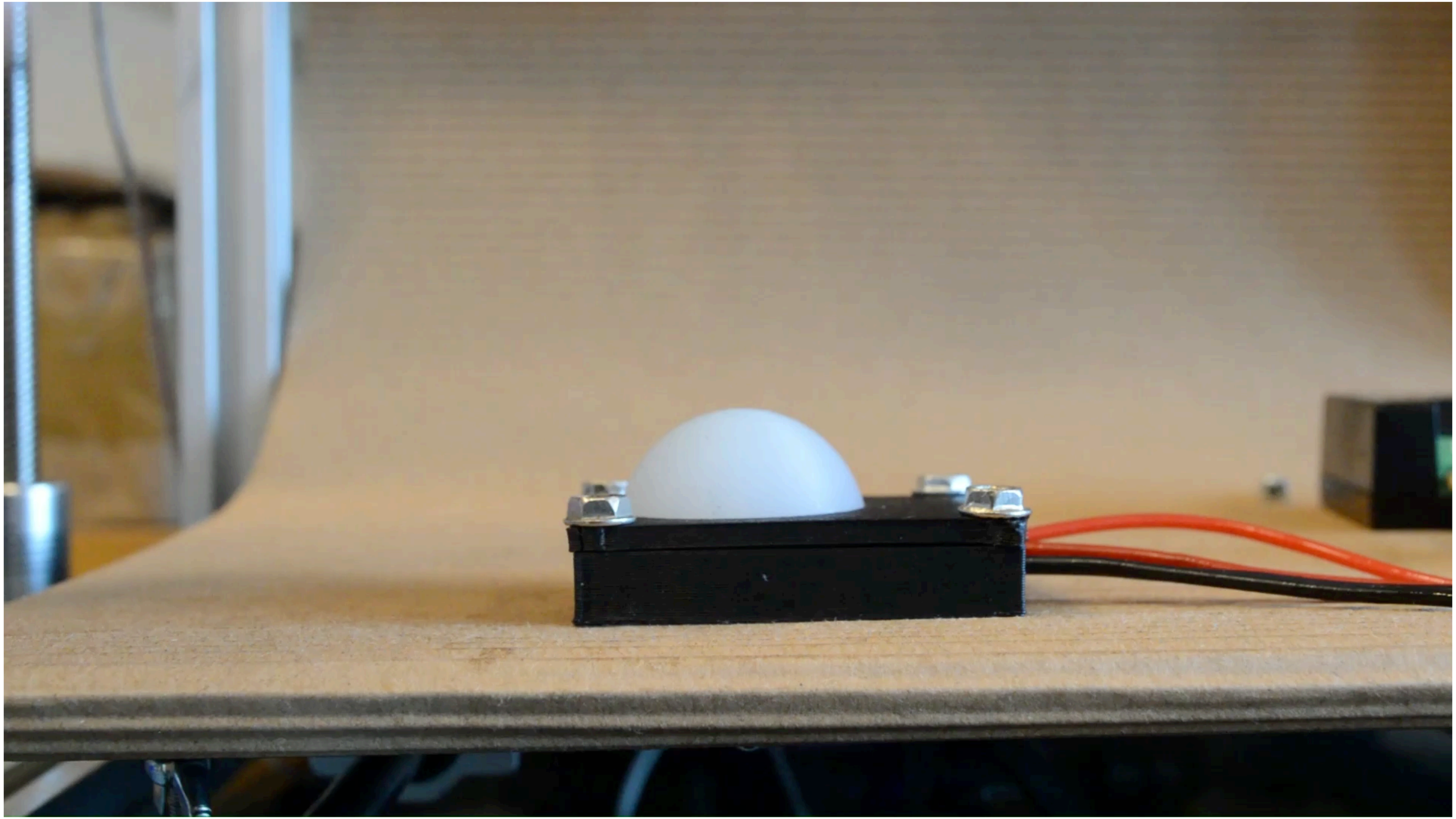

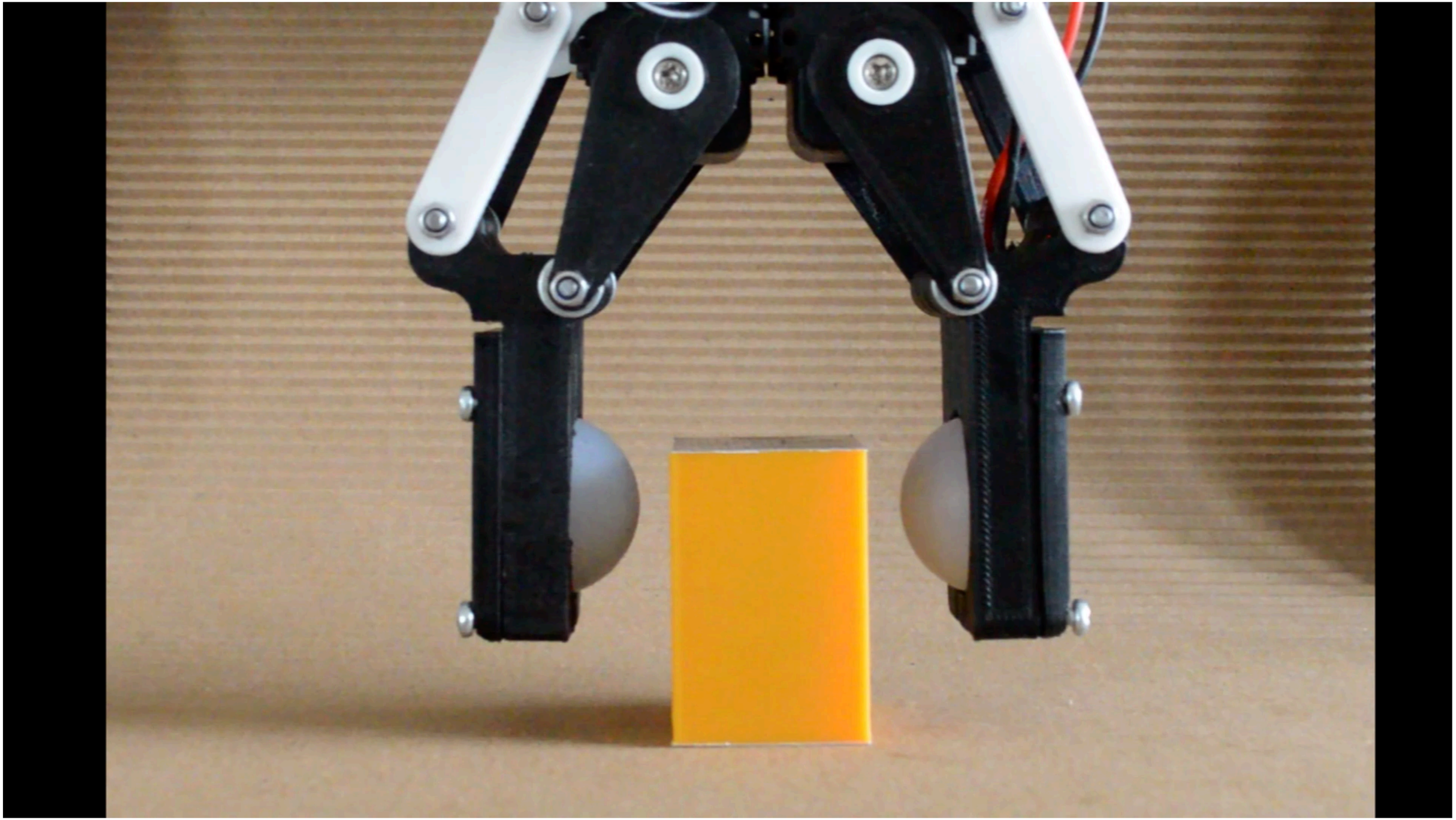

Table 1. Summary of Sensor Characteristics

Sensors	*Advantages*	*Disadvantages*
Rectangular beam	Quasi-linear response with shear strain	Low sensitivity
Cap with semicircumference circuit	Threshold response to indentation	Nonmonotonic response
Cap with sinusoidal circuit	Monotonic response and high sensitivity	—
Cap with multiple semicircumferential circuit	Threshold response with selectable onset	Nonmonotonic response
Cap with radial circuit	Enhanced sensitivity to axial compression	Linear response
Cap with two semiarches circuits	Sensitive to both compression and shear; good linearity	Low sensitivity to compression compared to shear

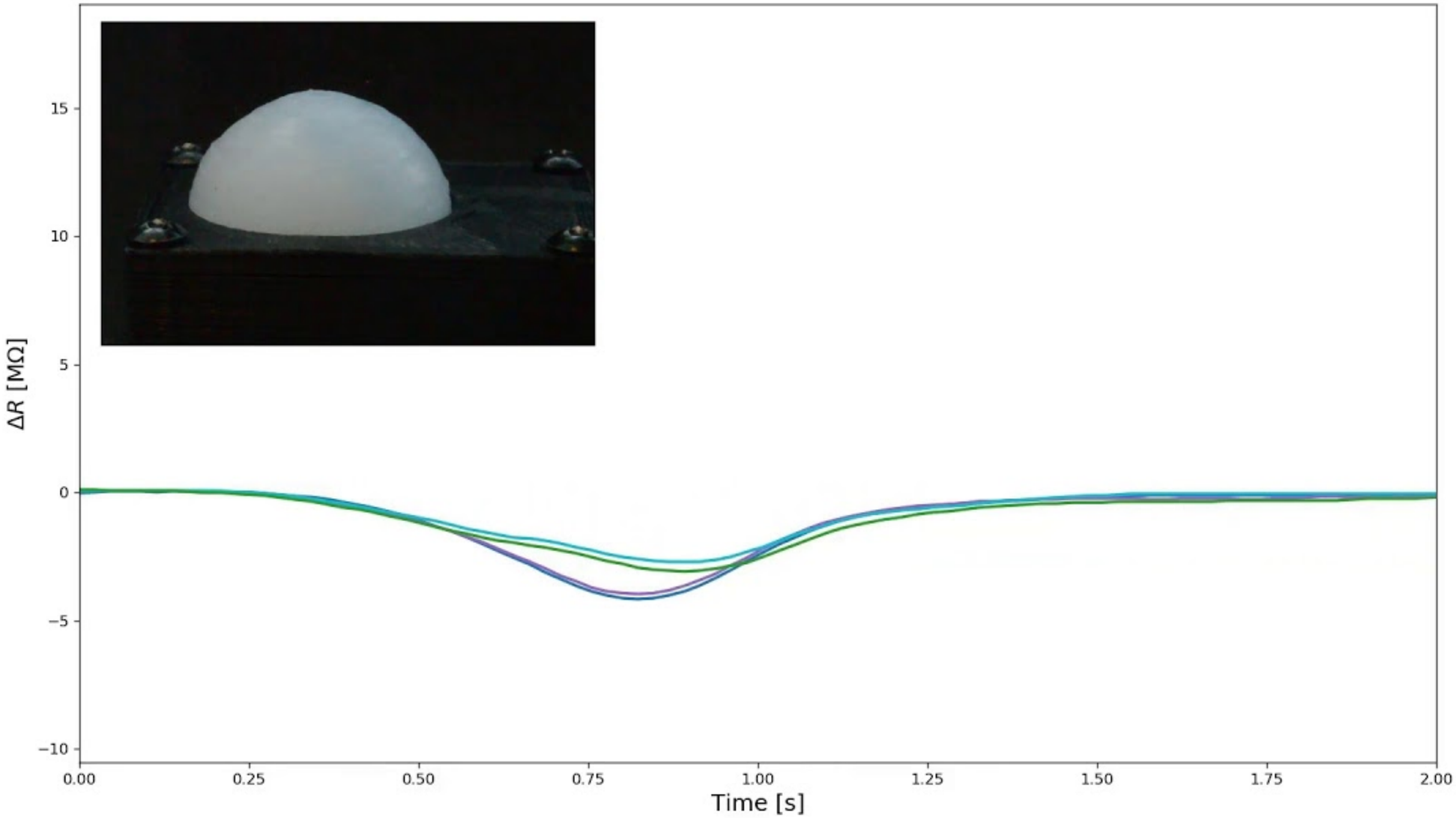
15
10
5
0
−5
−10
ΔR [MΩ]
0.00
0.25
0.50
0.75
1.00
1.25
1.50
1.75
2.00
Time [s]

ReSkin: versatile, replaceable, lasting tactile skins

Raunaq Bhirangi*, Tess Hellebrekers*, Carmel Majidi, Abhinav Gupta

https://reskin.dev/

Abstract: Soft sensors have continued growing interest because they enable both passive conformal contact and provide active contact data from the sensor properties. However, the same properties of conformal contact result in faster deterioration of soft sensors and larger variations in their response characteristics over time and across samples, inhibiting their ability to be long-lasting and replaceable. ReSkin is a tactile soft sensor that leverages machine learning and magnetic sensing to offer a low-cost, diverse and compact solution for long-term use. Magnetic sensing separates the electronic circuitry from the passive interface, making it easier to replace interfaces as they wear out while allowing for a wide variety of form factors. Machine learning allows us to learn sensor response models that are robust to variations across fabrication and time, and our self-supervised learning algorithm enables finer performance enhancement with small, inexpensive data collection procedures. We believe that ReSkin opens the door to more versatile, scalable and inexpensive tactile sensation modules than existing alternatives.

5th Conference on Robot Learning (CoRL 2021), London, UK.

Good tactile skins should provide

- Conformal contact
- Accurate compression and shear force
- High force resolution (<0.1N)
- High temporal resolution (>100Hz)
- Large surface area coverage (>4cm^2) with good spatial resolution
- Compact
- Inexpensive
- Long lasting

Cameras are bulky and slow (30-60Hz)

Resistive, capacitive, and piezoelectric sensors require many connections

Commercial solutions like BioTac are expensive (>$1000)

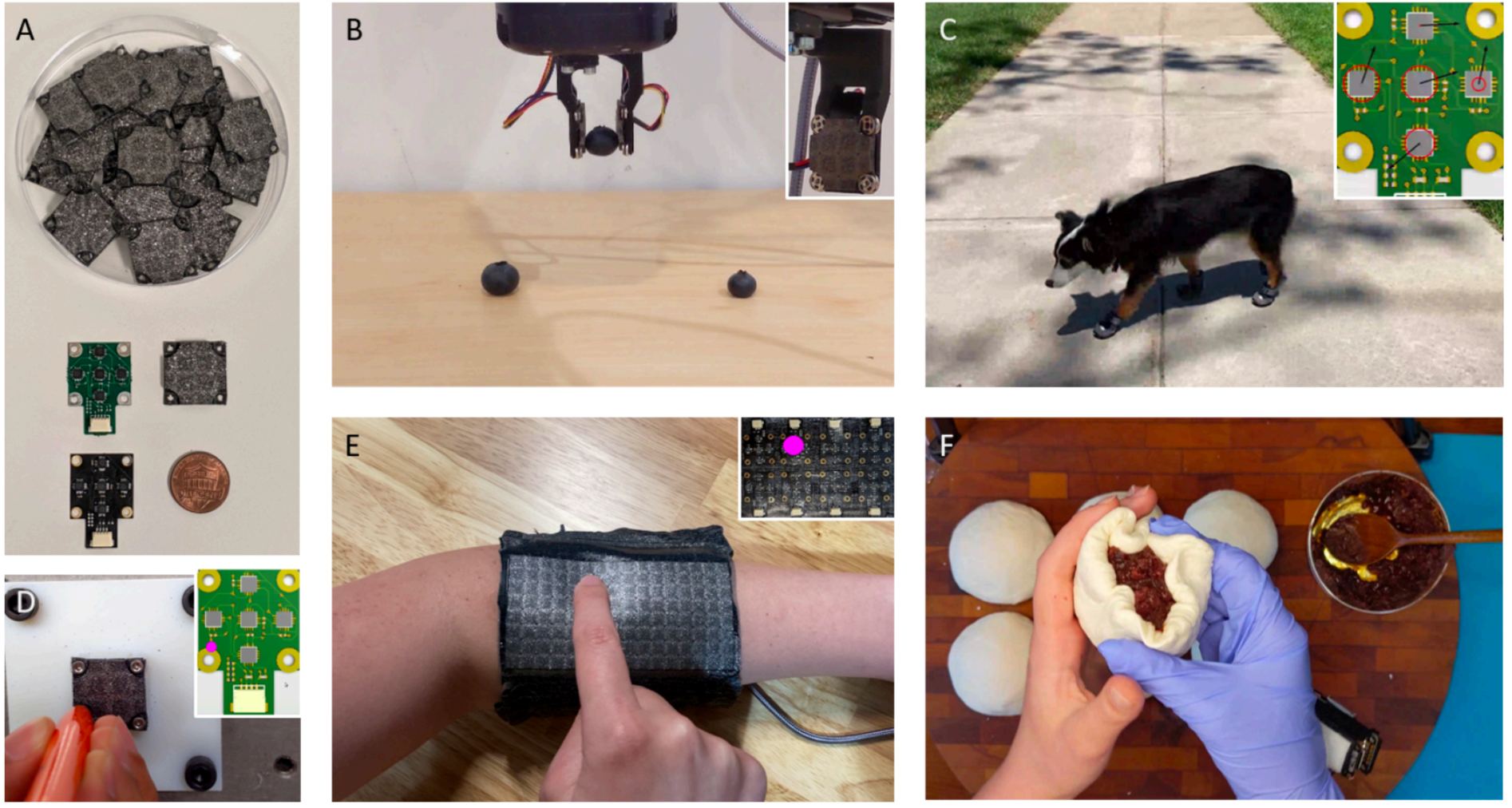

Figure 1: A) ReSkin is easy to fabricate and the size of a penny, enabling a wide range of applications. B) Robot gripper using tactile feedback from ReSkin sensors to hold a blueberry without squishing it. C) Dog shoe with an embedded ReSkin sensor; (inset) visualization of sensor measurements. D) Contact localization on a new ReSkin sensor using our self-supervised adaptation procedure. E) Contact localization on a ReSkin curated into a fabric sleeve as a 2in x 4in contiguous skin. F) ReSkin sensor as a fingertip sensor to record forces and contacts while folding a dumpling

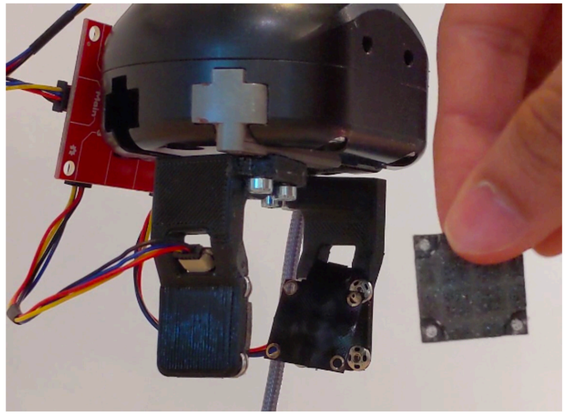

Figure 2: ReSkin is replaceable!

	ReSkin	DIGIT[1]	GelSlim [22]	BioTac [27]	RSkin [21]
Type	Magnetic	Optical	Optical	MEMS	Piezoresistive
Frequency	**400Hz**	60 Hz	60 Hz	100 Hz	?
Variable Form Factor	✓	✗	✗	✗	✓
Thickness <3mm	✓	✗	✗	✗	✓
Low Cost	✓	✓	✓	✗	✗
Easily replaceable	✓	✓	✓	?	✗
Area coverage	✓	✗	✗	✗	✓
Durable (>50k contacts)	✓	?	✗	✓	?

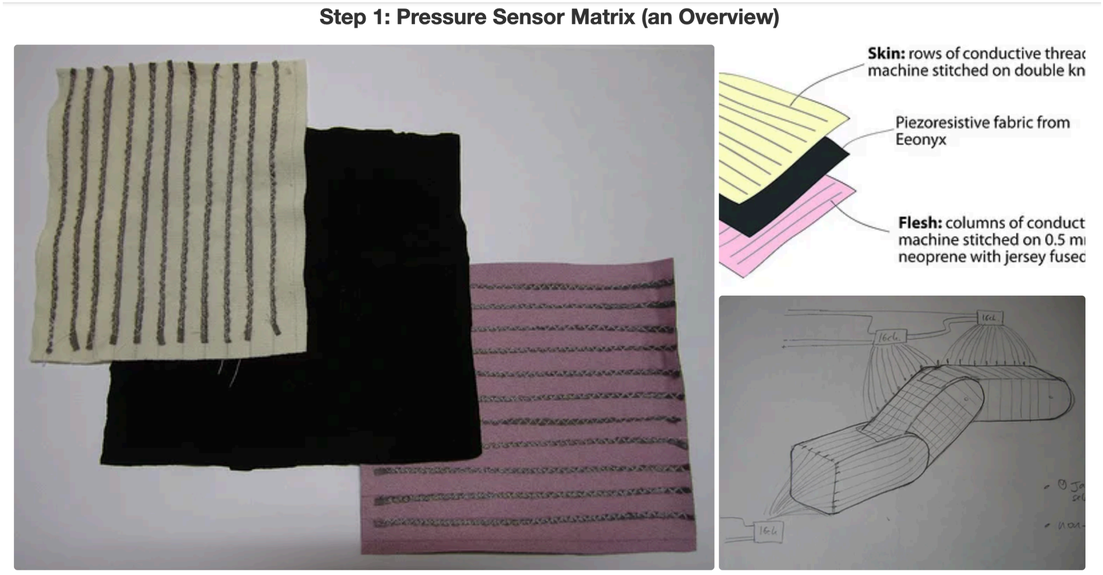

https://www.instructables.com/rSkin-Open-Source-Robot-Skin/

Stretchy piezoresistive fabric is sandwiched between the conductive rows and columns, and acts as a pressure sensitive layer. Piezoresistive materials have the property that their electrical resistance decreases under under mechanical stress, such as pressure.

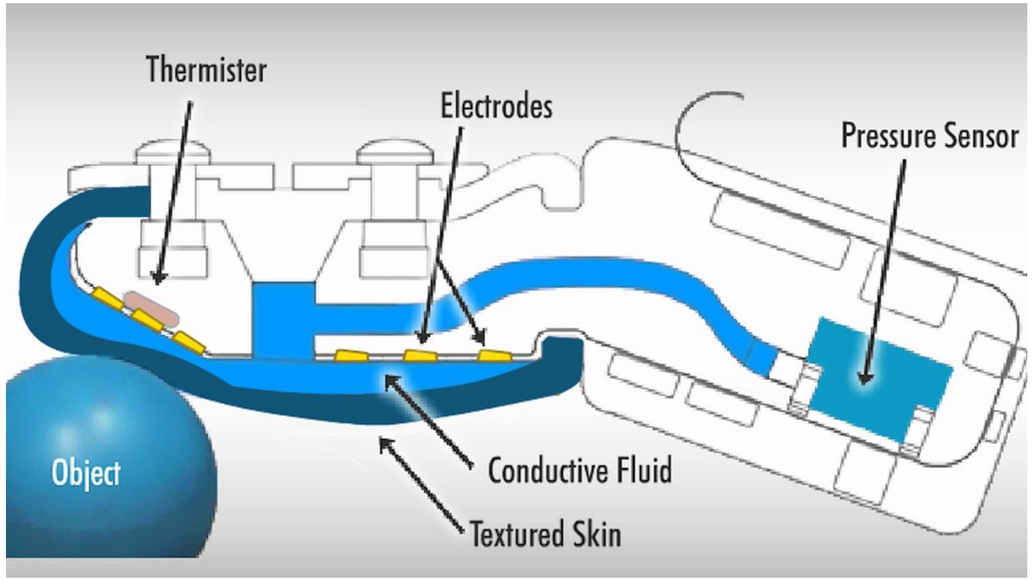


6X
SCOUT
OHAUS
Mix again for at least 30 seconds

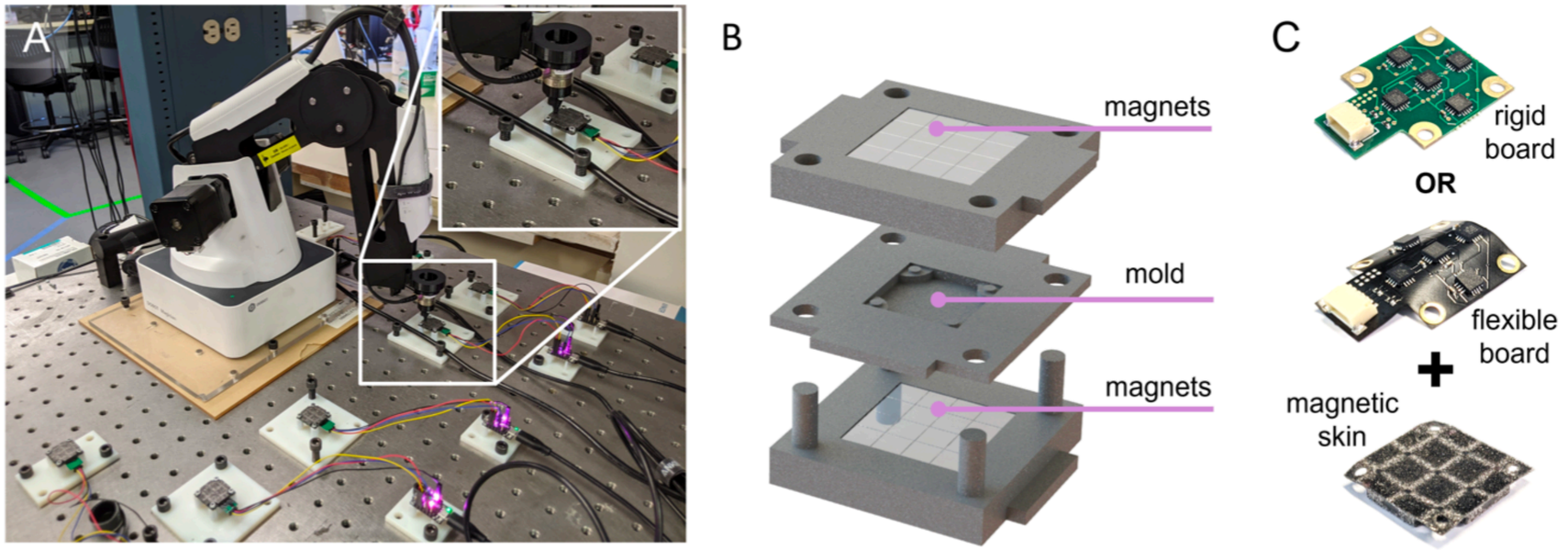

Figure 3: A) Experimental setup for data collection with Dobot Magician, ATI Nano 17 (inset), and six sensor boards streaming to a control computer. B) Mold for curing elastomer along with magnet holders. C) Two types of circuit boards – rigid and flexible – designed to be used with ReSkin.

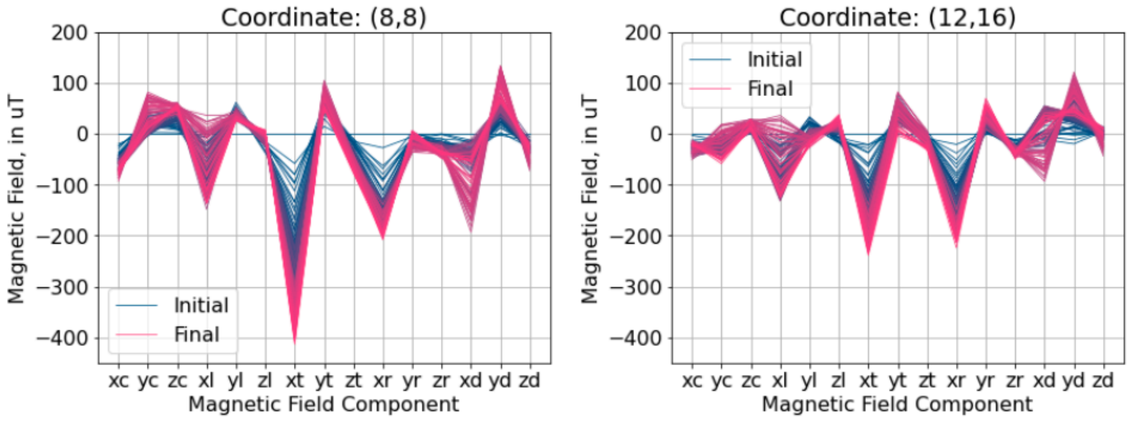

(a) Variation of magnetic field over time for a single sensor at two different points, over 10,000 indentations. The first measurement is subtracted from other measurements to better illustrate degree of variation.

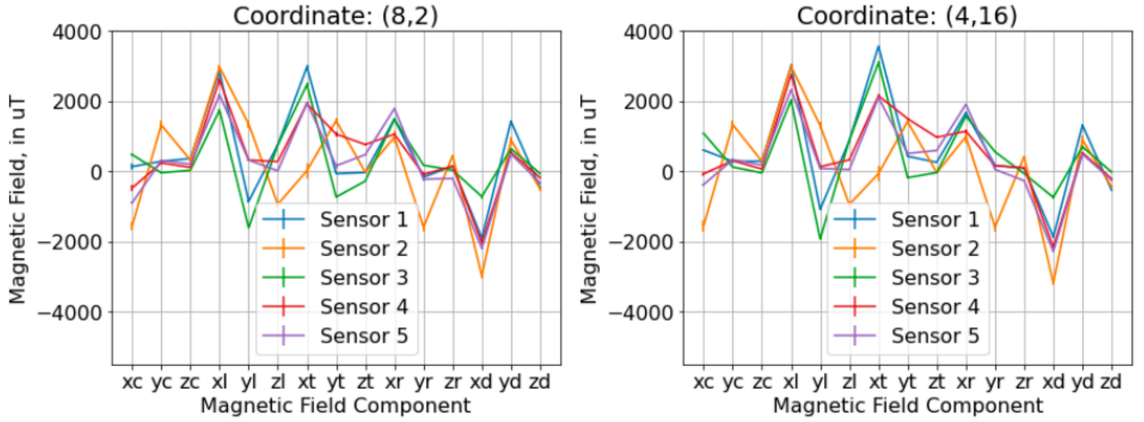

(b) Variation in magnetic field at two different points across five different sensors. Each line corresponds to the average magnetic field measured over 10,000 indentations for a particular sensor

Figure 4: Variation in magnetic field over time and across different sensors. Each tick on the x-axis corresponds to a component of the magnetic fields measured by the sensor. While the general properties of the individual sensors overlap, there is still obvious variation across the samples.

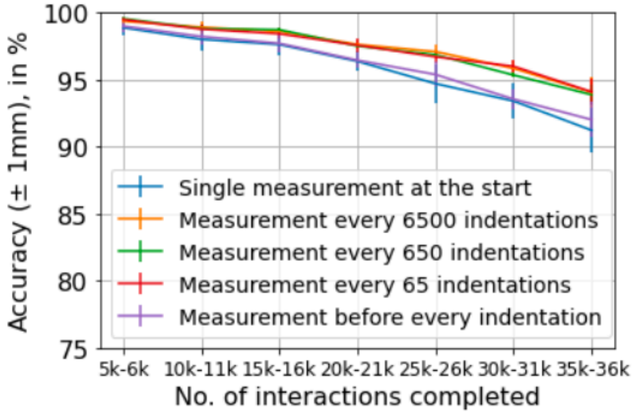

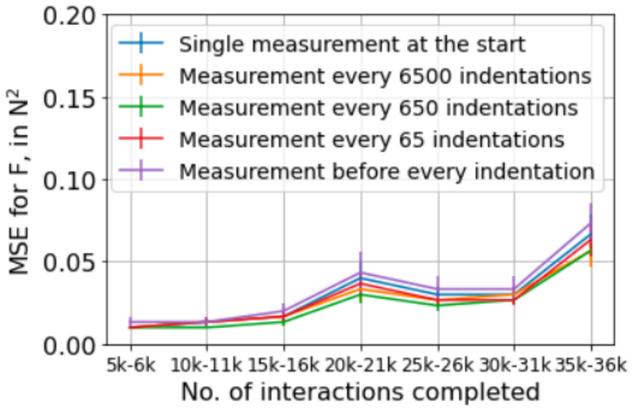

(a) Accuracy of contact localization and MSE for force predictions, as the number of interactions with the skin increases

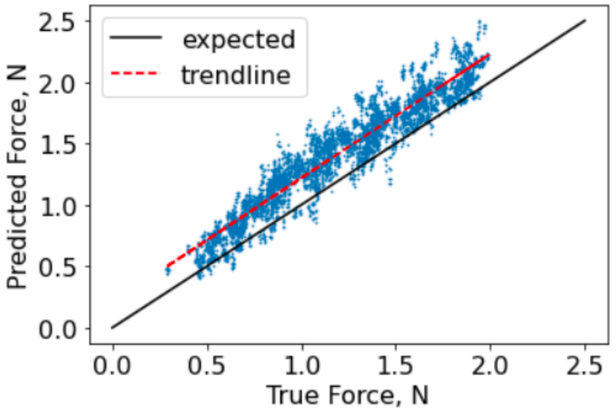

(b) Scatter plot of predicted force and the actual force applied, after 45,000 interactions.

Figure 5: Model performance with increasing number of interactions

input = magnetic flux from 5 magnetometers

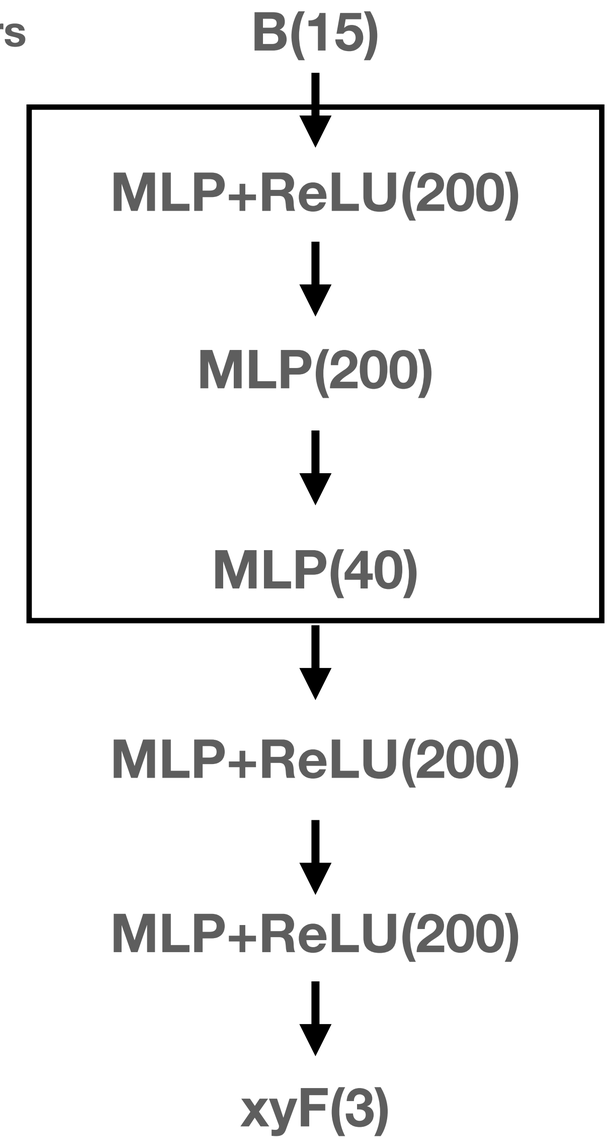

feat(.) = feature extraction network

output = position(x,y) and force(fx,fy,fz)

We use two techniques to help improve generalization for new skins and PCBs. First, instead of using data from a single sensor, we use data from multiple sensors to train our mapping function. This allows the model to see more diverse data in training and learn a more generalizable mapping function. Additionally, we apply a feature regularization component (self-supervised loss) to our loss function. This component is a triplet loss computed in feature space as follows:

$$\mathcal{L}_{\text{triplet}} = \max\left(0, ||feat(\mathbf{B}_a) - feat(\mathbf{B}_p)||^2 - ||feat(\mathbf{B}_a) - feat(\mathbf{B}_n)||^2\right), \quad (1)$$

where $\mathbf{B}_a, \mathbf{B}_p$ and $\mathbf{B}_n$ are three datapoints with corresponding contact locations $\mathbf{x}_a, \mathbf{x}_p$ and $\mathbf{x}_n$, such that $||\mathbf{x}_a - \mathbf{x}_p|| < ||\mathbf{x}_a - \mathbf{x}_n||$, ie. $\mathbf{x}_a$ is closer to $\mathbf{x}_p$ than $\mathbf{x}_n$. Subscripts a, p and n refer to anchor, positive and negative samples respectively. This loss encourages points that are closer on the skin to be closer to each other in feature space. It acts as a regularizer while also enabling us to use the self-supervised adaptation procedure described in the following paragraph.

Note that this self-supervised loss does not require ground-truth contact location or force readings and therefore can be leveraged to further improve performance on new sensor boards and skins. A new user can collect their own unlabeled dataset, which can be indexed without requiring explicit labels. For instance, the user can use the tip of a pen to indent the sensor skin in a straight line and incrementally index these points as they move along the line. Triplets of points can now be sampled along this line, and the indices can be used to order the pairs within each triplet by distance. Our multi-sensor learned model can then be fine-tuned using these triplets to minimize the triplet loss. At every training step, we sample a batch from the original training data, and an equal-sized batch of triplets (sampled with replacement) from the unlabeled dataset. The former is used to minimize the original loss function, while the latter is only used to minimize the triplet loss.

Model	Accuracy, in %	MSE_{xy}, in mm^2	MSE_F, in N^2
Single-sensor	25.24±10.12	6.453±3.363	0.420 ± 0.149
Multi-sensor without triplet loss	84.43±12.88	0.733±0.707	0.155 ± 0.025
Multi-sensor with triplet loss	81.03±12.86	0.756±0.718	0.155 ± 0.030
Multi-sensor with triplet loss, adapted using 390 indentations	$\mathbf{87.00 \pm 11.81}$	$\mathbf{0.514 \pm 0.601}$	$\mathbf{0.142 \pm 0.025}$

Table 2: The single-sensor baseline performs poorly, failing to capture variability across sensors. Our self-supervised adaptation significantly improves prediction accuracy as well as MSE in xy, F

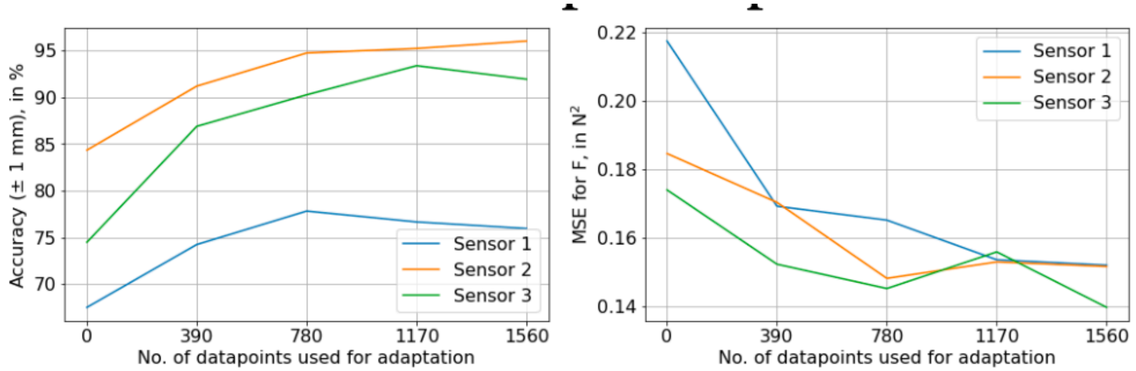

(a) Self-supervised adaptation improves significantly even with small quantities of adaptation data

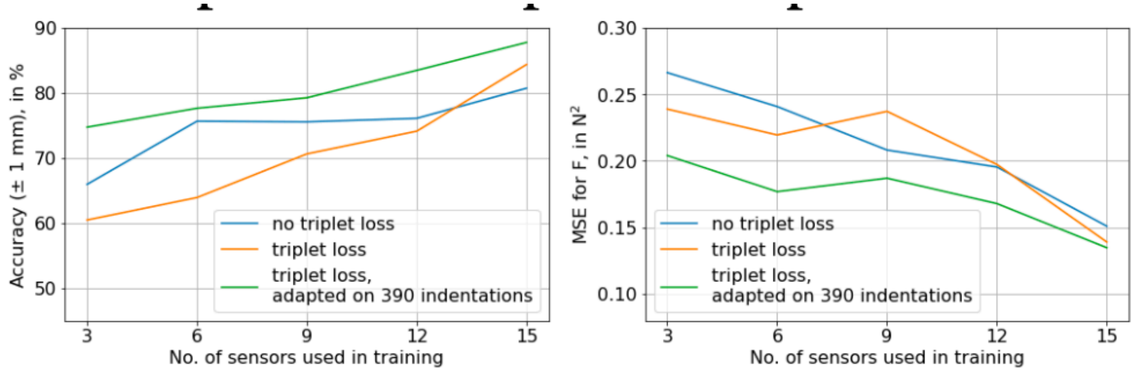

(b) Self-supervised adaptation leads to even larger performance gain with fewer sensors in training data

Figure 6: Self-supervised adaptation works with lesser adaptation data as well as training data

ReSkin: a versatile, replaceable, low-cost skin for AI research on tactile perception

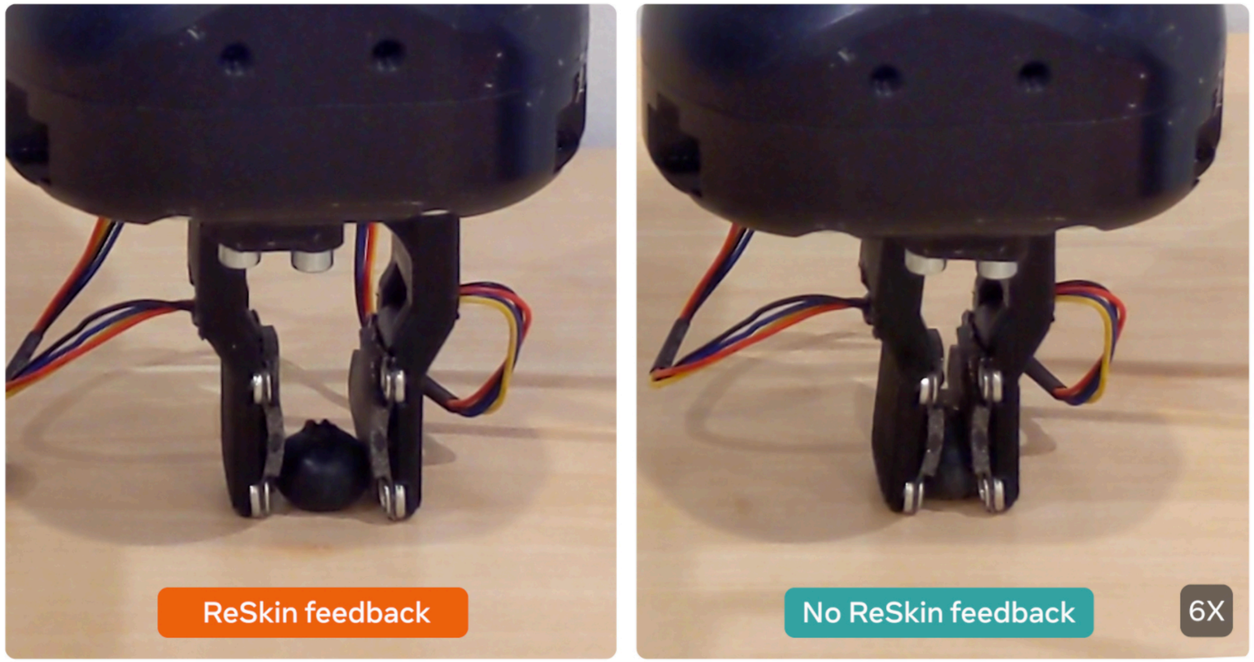

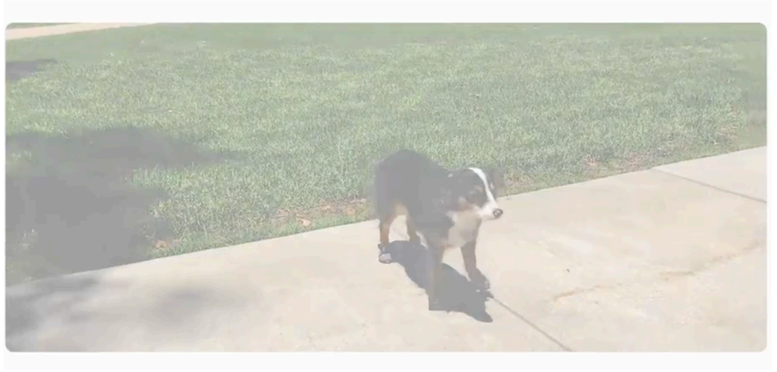

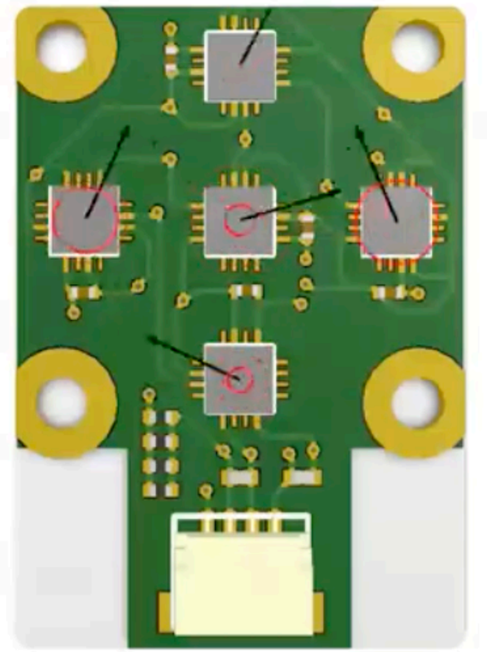

Our sense of touch helps us navigate the world around us. With it, we can gather information about objects — such as whether they're light or heavy, soft or hard, stable or unstable — that we use to accomplish everyday tasks, from putting on our shoes to preparing a meal. AI today effectively incorporates senses like vision and sound, but touch remains an ongoing challenge. That's in part due to limited access to tactile-sensing data in the wild. As a result, AI researchers hoping to incorporate touch into their models struggle to exploit richness and redundancy from touch sensing the way people do.

https://ai.facebook.com/blog/reskin-a-versatile-replaceable-low-cost-skin-for-ai-research-on-tactile-perception

https://www.youtube.com/watch?v=Vrk4YMbRhac